Numerical Study of the High-Speed Bypass Effect on a Plate-Fin Type Heat Exchanger

Minsung Kim[a], Man Yeong Ha[a] and June Kee Min[b]*
*Author for correspondence
[a] School of Mechanical Engineering,
[b] Rolls-Royce and Pusan National University Technology Centre in Thermal Management,
Pusan National University, 2, Busandaehak-ro 63beon-gil, Busan 46241, South Korea
E-mail: kms514v@pusan.ac.kr

ABSTRACT

Heat exchangers having a bypass stream have wide ranging engineering applications such as heat sinks for electronics cooling. Due to their operating conditions, studies on the effect of the bypass region on the aero-thermal performance of heat exchangers have usually focused on the low-speed flow regime. Recently, however, the need for research on the high-speed bypass effect is increasing, especially in connection to aero-engine applications. The surface cooler, which is mounted on the fan casing of an aero-engine, uses a cold bypass stream to dissipate the heat from the oil system or the power generator devices of the engine. In this paper, a fundamental numerical study to evaluate the aero-thermal characteristics of a fin-type heat exchanger having a bypass duct under high-stream operating conditions has been conducted. A simplified bypass duct model has been used to formulate new performance correlations of the pressure drop and heat transfer coefficient by varying the bypass ratio and other important geometric parameters. The tested Mach number of the bypass stream was as high as 0.6. The obtained results are compared with previous low-speed correlations in both qualitative and quantitative terms. The newly summarized correlations could be useful for the preliminary design of heat exchangers for high-speed operating conditions in the early stage of the heat exchanger design. Comparison between the flow-network analysis results and the two-dimensional calculations showed the advantage of using the new correlations.

INTRODUCTION

The demand for more environmentally friendly airplanes has created a demand for aero engines with sharply increased efficiency. The specific fuel consumption (SFC) of the gas-turbine engine is highly related to the operating pressure ratio (OPR) and the turbine inlet temperature (TIT). In order to achieve high efficiency using an advanced cycle, equipment with an ultra-light heat exchanger is essential. This is because high efficiency aero-engines require a heat exchanger with a minimal weight penalty and high aero-thermal performance. Min et al. [1] reviewed existing and possible candidate heat-exchange technology for use in recuperator, intercooler, and cooling-air cooler applications. Increasing the bypass ratio (BPR) of the engine is another method by which to increase the efficiency of turbo-fan engines. In this case, the heat from the corresponding oil system, such as the gear box and generator in the transmission system, should be dissipated using various oil coolers. Kim et al. [2] studied the effect of cooler installation location in a high-speed aero engine with a plate fin. A number of studies aimed at enhancing aerothermal performance by varying the fin-shape of the heat exchanger have been reported. It was found that a modified fin surface may have a high heat transfer coefficient, but that its pressure drop may be excessive for wide application.

In the present study, the influence of bypass height and Mach number on the aero-thermal performance of the cooler was investigated numerically. To improve the efficiency of the calculations, the fundamental pressure drop and heat transfer characteristics were investigated using an idealized, channel-shaped computational domain of two dimensions.

NOMENCLATURE

C_p	[J/kgK]	*Specific heat*
f	[-]	Fanning friction factor
G_v	[-]	Volume goodness factor
G_a	[-]	Area goodness factor
H	[mm]	Bypass height
h	[mm]	Fin height
h_{air}	[W/m^{2}K]	Heat transfer coefficient
k	[W/mK]	Thermal conductivity
L	[mm]	Domain length
l	[mm]	Fin length
Ma	[-]	Mach number
Nu	[-]	Nusselt number
P	[Pa]	Static pressure
Q	[W]	Heat transfer rate
R	[m^{2}K/W]	Thermal resistance
Re	[-]	Reynolds number
Pr	[-]	Prandtl number
St	[-]	Stanton number
T	[K]	Static temperature
U	[W/m^{2}K]	Overall heat transfer coefficient
u,v,w	[-]	Dimensionless velocity components in x, y and z direction
V_{avg}	[m/s]	Average velocity
V_{mag}	[m/s]	Velocity magnitude
x_i	[-]	Cartesian coordinate system

Greek symbols

α	Thermal diffusivity
μ	Fluid viscosity
ν	Fluid kinematic viscosity
ρ	Fluid density
τ	Shear stress
Υ	Porosity

Subscripts

i,j	Tensor notation

NUMERICAL METHODOLOGY

Figure 1 shows the computational model and boundary conditions for the two-dimensional unit-fin model used in the present study. No-slip conditions are imposed on the top and bottom surfaces. Velocity inlet and pressure outlet conditions are applied on the inlet and outlet boundary regions, respectively. In this study, the porous media approximation is used for the plate-fin heat exchanger. This approximation is convenient since it not only simplifies the complex geometrical problems and improves the computational efficiency but also obtains reasonable predictions. The thermal boundary condition considered in the present study is the conjugated heat transfer (CHT) condition. In order to calculate the conjugated heat transfer between the hot cooler surface and ambient cold air flow, the thermal conditions in the oil side of the oil passage were modelled by the average temperature and constant heat transfer coefficient.

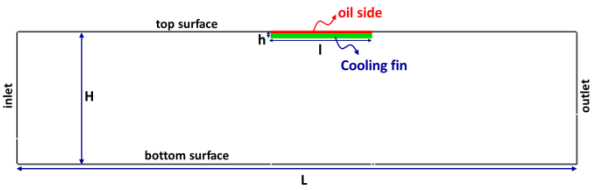

Figure 1 Computational domain and boundary conditions

The flow length is set to 2,000 mm and the bypass height (H) is a design parameter that is varied as 125, 225, 325, 425, and 525 mm. The fin height (h) and fin length (l) are 25 mm and 400 mm, respectively. A structured hexahedral mesh is generated in the computational domain. The grid is carefully distributed near the wall, in particular at the cooling fin and the surface of the oil passage, in order to resolve the high velocity and temperature gradients. Based on the grid dependency test, the number of grid cells distributed in the computational models is approximately 70 thousand. The second order upwind scheme was used for spatial discretization, and the pressure-based coupled scheme was used for pressure-velocity coupling.

Assuming the air as an ideal gas, the continuity, momentum, and energy equations describing the present study, compressible, and turbulent flows are given in Eqs. (1) – (3).

$$\frac{\partial}{\partial x_i}\left(\rho u_i\right) = 0 \tag{1}$$

$$\frac{\partial}{\partial x_j}\rho u_i u_j = -\frac{\partial P}{\partial x_i} + \frac{\partial}{\partial x_j}\left[\mu\left(\frac{\partial u_i}{\partial x_j} + \frac{\partial u_j}{\partial x_i}\right) - \overline{\rho u'_i u'_j}\right] \tag{2}$$

$$\frac{\partial}{\partial x_i}\left(\rho C_p u_i T\right) = -\frac{\partial}{\partial x_i}\left(-k\frac{\partial T}{\partial x_i} + \rho C_p \overline{u'_i T'}\right) \tag{3}$$

where the subscripts (i and j) represent the tensor notation (i = 1, 2, 3 and j = 1, 2, 3). In Eqs. (1) – (3), u_i, P, and T denote the velocity vector, static pressure, and temperature, respectively. ρ, μ, k, and C_p in Eqs. (1) – (3) represent the fluid density, viscosity, thermal conductivity, and specific heat, respectively. All variables are time-averaged mean values, and Eqs. (1) – (3) are compressible Reynolds-averaged Navier-Stokes (RANS) equations. In this work, the commercial computational fluid dynamics (CFD) software FLUENT is used to simulate the fluid flow in the domain. For the turbulent flow, the standard k-ε model with an enhanced wall function was adopted. The Mach number in the core of the bypass duct of the domain is approximately 0.29 to 0.65, which includes the subsonic region. A second-order upwind scheme is adopted for the spatial discretization of the transport equations of the momentum, energy, and turbulent quantities.

In this calculation, the bypass height (H) at the inlet of the computational domain was chosen for the reference length, and the average velocity V_{avg} on the inlet boundary for the reference velocity. The range of average inlet velocity (V_{avg}) was from 100 m/s to 220 m/s and had 10 increments. The average temperature of the inlet air was 293 K for the channel model. For the oil side, the mean temperature of the oil and the corresponding heat transfer coefficient were given as 386 K and 2000 W/m^{2}K, respectively. The averaged fluid properties were also used for the calculation of dimensionless variables. Using these variables, the Reynolds number is defined as

$$\mathrm{Re} = \frac{V_{avg} H}{\nu} \tag{4}$$

where ν is the kinematic viscosity. The Prandtl number is

$$\mathrm{Pr} = \frac{\nu}{\alpha} \tag{5}$$

where α is the thermal diffusivity.

The Fanning friction factor f, Nusselt number Nu, Stanton number St, and Colburn j factor are defined as follows:

$$f = \frac{\left(\Delta P / L\right) H}{2\rho V^2_{avg}} \tag{6}$$

$$Nu = \frac{h_{air} D_h}{k} \tag{7}$$

$$St = \frac{Nu}{\mathrm{Re}\,\mathrm{Pr}} \tag{8}$$

$$j = St\,\mathrm{Pr}^{2/3} \tag{9}$$

In Eqs. (6) – (9), $\Delta P / L$ is the average pressure gradient in the stream-wise direction and h_{air} the heat transfer coefficient. The volume and area goodness factor [5] are defined by

$$G_v = \frac{St}{f^{1/3}} \tag{10}$$

$$G_a = \frac{j}{f} \tag{11}$$

For a given pumping power, a larger volume goodness factor yields a smaller heat-transfer surface area, resulting in a smaller heat-exchanger matrix volume, and a larger area goodness factor yields a smaller frontal area for the heat exchanger matrix [5]. In the design of a heat exchanger for an aero engine, both goodness factors should have equal importance due to the importance of the weight penalty and spatial installation limit. In this study, volume and area goodness factors are adopted for the evaluation of the fundamental aero-thermal performance of each bypass height using the channel model calculation.

In this study, the two-dimensional porous media approximation was conducted to calculate the performance of the heat exchanger. The porous media approximation is convenient since it not only simplifies the complex geometrical problems and improves the computational efficiency but also obtains reasonable predictions. Therefore, the two-dimensional model using this approximation is a good alternative to the current model of a plate-type heat exchanger when dealing with various engineering problems for a short-term research period. Figure 2 schematically illustrates the two-dimensional porous media model for the present study. Figure 3 provides detailed information of the fin specifications of the porous zone. As shown in this figure, the thickness of the fin and the length of the pitch were assumed as 0.8mm and 3.2 mm, respectively. The porosity (Υ) was assumed as 0.8, which is obtained by dividing 3.2 by 4.0.

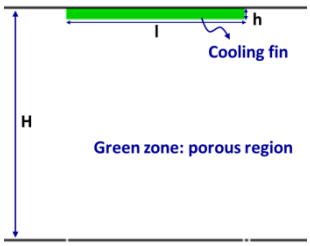

Figure 2 Schematic illustration of the 2D porous model for the present study

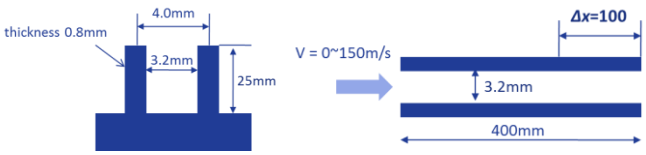

Figure 3 Detailed information of fin specifications of the porous zone

Figure 4 shows the results for the pressure drop in the considered inlet velocities. Using Eqs. (12) – (13), the coefficients of the porous media approximation for the present study were calculated as shown in Table 1. The term $\frac{\mu}{\alpha}v_i$ is Darcy's law in porous media and the term $C_2\frac{1}{2}\rho|v|v_i$ is the inertial loss in porous media.

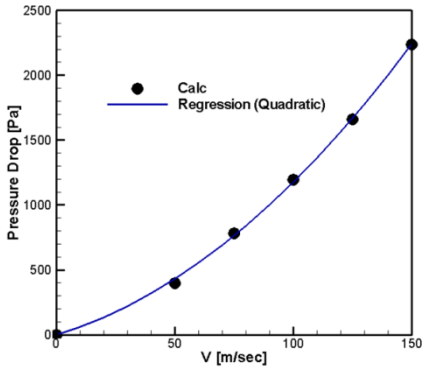

Figure 4 Results for the pressure drop in various inlet velocities

$$\frac{\partial P}{\partial x_i} = -\left(\frac{\mu}{\alpha}v_i + C_2\frac{1}{2}\rho|v|v_i\right) \quad (12)$$

$$\Delta P = Z_1 v + Z_2 v^2 \quad (13)$$

Table 1 Coefficients of porous media approximation for the present study

Coefficients	Values
Z_1	0.0634
Z_2	5.4241
$1/\alpha$	3.1720E+06
C_2	2.0336

RESULTS AND DISCUSSION

The accuracy of the present study was validated using previous experimental studies. Figure 5 shows a comparison of the computational results with the experimental data by Jonsson and Moshfegh [3]. This is similar to the present channel-model calculation except for the existence of the bypass region in the experiment. Detailed dimensions of the problem are represented in Figure 5(a). The calculation results and the experimental data showed good agreement, showing less than a 9.0% difference for the pressure drop and a 7.5% difference for the thermal resistance at a Reynolds number of 12,000. The variation of the pressure drop and the thermal resistance of the plate-fin type heat exchanger is also well captured in the numerical prediction.

Table 2 Detailed design space for the bypass height study

Cases	Bypass height (H) (mm)
Case 01	525
Case 02	425
Case 03	325
Case 04	225
Case 05	125

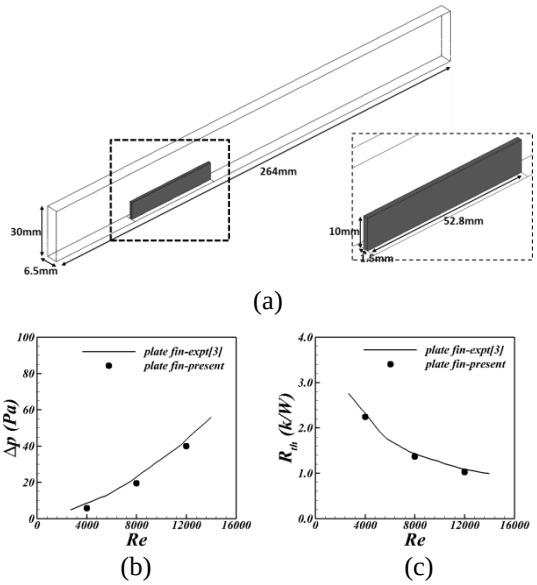

Figure 5 Comparison of calculation results with experimental data for fins in channel: (a) geometry, (b) pressure drop, and (c) thermal resistance

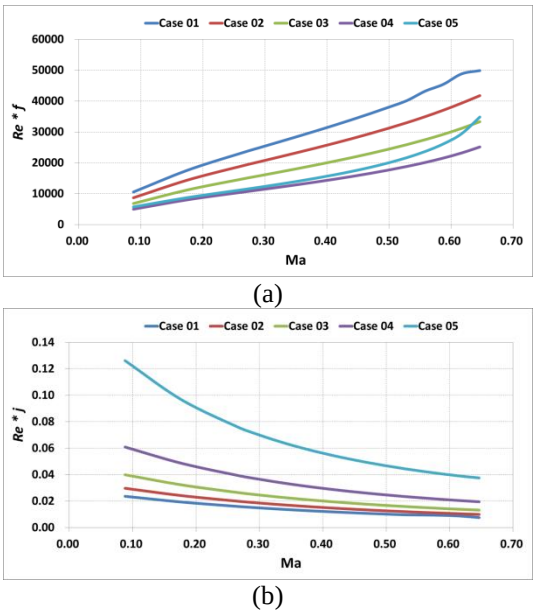

Figure 6 Results of the study on various bypass heights as a function of Mach number: (a) Reynolds number*friction factor, and (b) Reynolds number*Colburn *j*-factor

Table 2 presents the test matrix for the parametric study of the bypass height using the five calculation cases of the present study. The goal of this calculation is to find the optimal bypass height that can generate optimal aero-thermal performance considering the given heat transfer rate and pressure drop.

The values of the f·Re and j·Re correlations for the considered bypass height are plotted as a function of the Mach number in Figure 6. From Cases 01 to 05, f·Re increases due to increasing Mach number. For Case 05, the speed of air is higher than the other cases because of having a small inlet area. The case of short bypass height has a large shear stress on the bottom surface, and this can cause a large pressure drop between the inlet and the outlet. As shown in Figure 6(a), f·Re of Case 05 is significantly increased due to the increase in the Mach number.

The value of j·Re increases due to the decreased bypass height (H) at each Mach number. This is a result of the increasing air velocity around the SAOHE due to the decrease of the bypass height. For Cases 01 to 05, each correlation for f·Re and Mach number is obtained as follows:

$$f \cdot \mathrm{Re} = \mathrm{A} \cdot \mathrm{Ma}^3 + \mathrm{B} \cdot \mathrm{Ma}^2 + \mathrm{C} \cdot \mathrm{Ma} + \mathrm{D} \quad (14)$$

$$j \cdot \mathrm{Re} = \mathrm{A} \cdot \mathrm{Ma}^3 + \mathrm{B} \cdot \mathrm{Ma}^2 + \mathrm{C} \cdot \mathrm{Ma} + \mathrm{D} \quad (15)$$

The coefficients for A, B, C, and D of the f·Re and j·Re correlations are shown in Table 3 and Table 4, respectively. Theses correlations have the form of a cubic equation and they are a function of the Mach number. Note that the R^2 values of the f·Re and j·Re correlations are acceptable in terms of using these correlations to predict the heat exchanger performance. The R^2 value is over 0.98 in each correlation for the present study.

Table 3 Coefficient of f·Re correlations

A	B	C	D
132418	-129771	103171	2533.7
126830	-124889	89724	1709
111350	-105466	71071	1327.8
101719	-90749	53493	888.2
275744	-236031	90915	-968.6

Table 4 Coefficient of j·Re correlations

A	B	C	D
-0.0487	0.09	-0.0708	0.0293
-0.0453	0.096	-0.0844	0.0364
-0.0663	0.1389	-0.1178	0.0492
-0.1221	0.2438	-0.1943	0.0761
-0.3881	0.7048	-0.4894	0.1638

Figure 7 shows the distribution of the velocity magnitude on the surface of the computational domain at Ma = 0.4. As shown in this figure, the velocity magnitude increases around the fins due to the decrease in the bypass height. This is due to the reduction of the flow resistance resulting from the decreased inlet area. Figure 8 shows the results of the streamline pattern for the computational domain at Ma = 0.4. As shown in this figure, the streamline that is around the fin turns due to the increased bypass height. For Case 05, the streamline forms a straight line because of the no-slip condition on the bottom surface. The pressure on the surface of the computational domain is also increased due to the decreased bypass height, as shown in Figure 9. Figure 10 shows the distribution of temperature on the surface of the computational domain at Ma

= 0.4 for Case 01 to Case 05. For Cases 04 and 05, the heat transfer between the oil- and air-side increased more than the other cases because high-speed velocity around the fins. However, for Case 05, the pressure drop is larger compared to the values of Cases 01 to 04, respectively.

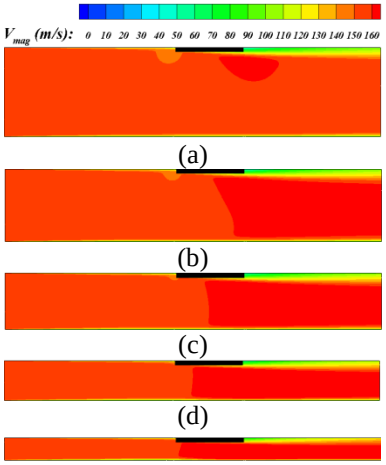

Figure 7 Distribution of velocity magnitude on the surface of the computational domain at Ma = 0.4: (a) Case 01, (b) Case 02, (c) Case 03, (d) Case 04, and (e) Case 05

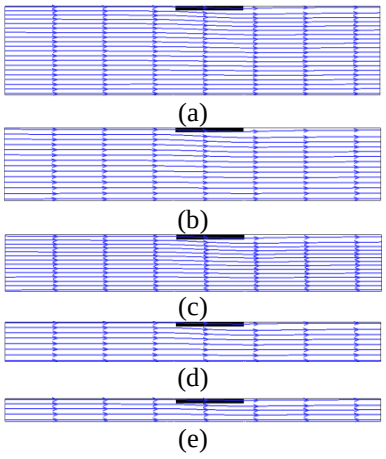

Figure 8 Results of streamline pattern for the computational domain at Ma = 0.4: (a) Case 01, (b) Case 02, (c) Case 03, (d) Case 04, and (e) Case 05

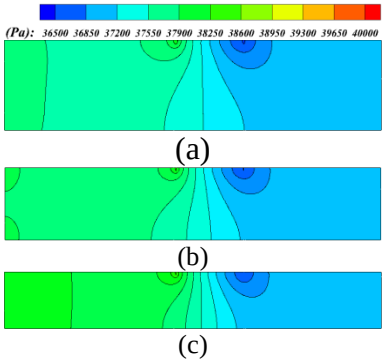

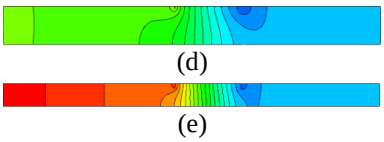

Figure 9 Distribution of pressure on the surface of the computational domain at Ma = 0.4: (a) Case 01, (b) Case 02, (c) Case 03, (d) Case 04, and (e) Case 05

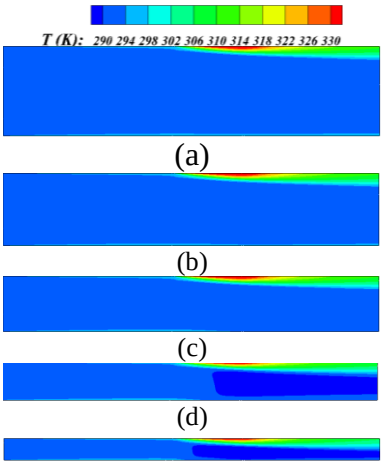

Figure 10 Distribution of temperature on the surface of the computational domain in Ma = 0.4: (a) Case 01, (b) Case 02, (c) Case 03, (d) Case 04, and (e) Case 05

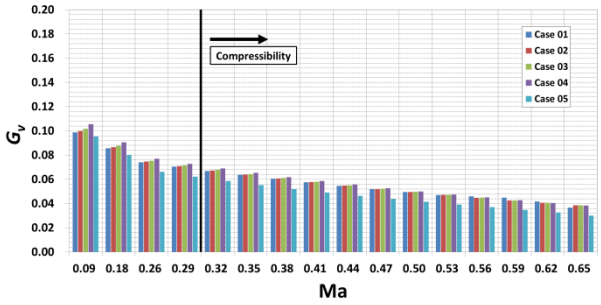

(a)

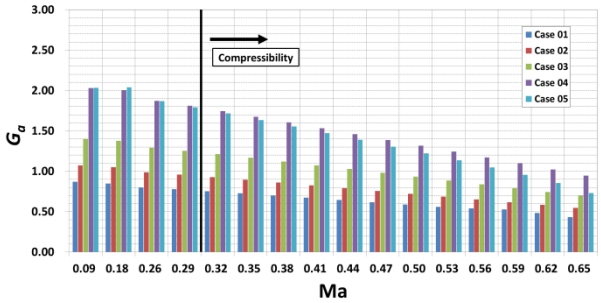

(b)

Figure 11 Results of the parametric study on various bypass heights: (a) volume goodness factor, and (b) area goodness factor

The comparison of volume and area goodness factors is summarized in Figure 11. As shown in this figure, the volume and area goodness factor decreased due to the increased Mach number, because the friction factor, which influences the compressibility effect, becomes larger due to the increased Mach number. The volume and area goodness factors do not show great improvement of the compactness in a subsonic flow field.

CONCLUSION

In this work, the flow and thermal characteristics of a plate-fin heat exchanger in a high speed bypass flow were investigated numerically. A two-dimensional compressible Navier-Stokes procedure to solve for the flow and heat transfer around the cooler was conducted using a unit-fin model with a planar boundary condition. The aero-performance of a plate-type heat exchanger for various bypass heights was assessed. Using a plate-fin heat exchanger, the basic performance metric, which includes the pressure drop and heat transfer, was evaluated using an idealized channel computational model. f·Re is increased due to the increase of the Mach number, whereas j·Re is decreased.

The correlations of f·Re and j·Re, which are functions of the Mach number, are represented in the form of cubic equations. Using these correlations, the one-dimensional calculation can be used to estimate the performance of heat exchanger under the defined fin specifications.

Further studies on the surface cooler, such as the effect of fin height and thickness, would be helpful, since the bypass ratio of modern aero-engines must be enlarged to increase engine efficiency and this causes the corresponding oil temperature in the transmission or gear box system to increase rapidly.

ACKNOLEDGEMENTS

This work was supported by a National Research Foundation of Korea (NRF) grant funded by the Korean government (MSIP) (No. NRF-2013R1A2A2A01067251).

REFERENCES

[1] J.K. Min, J.H. Jeong, M.Y. Ha, K.S. Kim, High temperature heat exchanger studies for applications to gas turbines, *Heat Mass Transfer*, Vol. 46, 2009, pp.175-186.

[2] S. Kim, J.K. Min, M.Y. Ha, C. Son, Investigation of high-speed bypass effect on the performance of the surface air–oil heat exchanger for an aero engine, *Int. J. Heat Mass Transfer*, Vol. 77, 2014, pp.321-334.

[3] H. Jonsson, B. Moshfegh, Modeling of the thermal and hydraulic performance of plate fin, strip fin, and pin fin heat sinks – Influence of flow by-pass, *IEEE Trans. Compon. Packag. Technol.*, Vol. 24, 2001, pp.142-149.

[4] M. Kim, M.Y. Ha, J.K. Min, A numerical study on various pin–fin shaped surface air–oil heat exchangers for an aero gas-turbine engine, *Int. J. Heat Mass Transfer*, Vol. 93, 2016, pp.637-652.

[5] R.K. Shah, A.L. London, Laminar Flow Forced Convection in Ducts, *Academic Press Inc*, New York, 1978.

[6] H. Jonsson, B. Moshfegh, Enhancement of the cooling performance of circular pin fin heat sinks under flow by-pass conditions, in: *Proceedings of the Eighth IEEE Inter Society Conference on Thermal Phenomena (ITHERM)*, San Diego, 2002, pp. 425-432.

[7] J.A. Ko, S.K. Kim, M.Y. Ha, J.K. Min, R. Stieger, S. Mason, J.H. Doo, C. Son, A study on the installation of the surface air–oil heat exchanger for the application to aero gas-turbine engine, *ISABE 2013*, Busan, 2013.

[8] J.C. Adams, Advanced heat transfer surfaces for gas turbine heat exchangers (PhD thesis), University of Oxford, 2004.

[9] N. Hasan, S. M. Khan, F. Shameem, A new flux-based scheme for compressible flows, Computers & Fluids, Vol. 119, 2015, pp.58-86.